Dissociative recombination of small carbon cluster cations

O. Heber
Department of Particle Physics, Weizmann Institute of Science, 76100, Rehovot, Israel

K. Seiersen, H. Bluhme, A. Svendsen, and L. H. Andersen
Department of Physics and Astronomy, University of Aarhus, DK-8000 Aarhus C, Denmark

L. Maunoury
CIRIL, Avenue Henri Becquerel, Boîte Postale 5133, 14070 Caen cedex 5, France
(Received 23 November 2005; published 14 February 2006)

The dissociative recombination of small cluster cations with free, zero-energy electrons was studied at the ASTRID storage ring. It was found that only two-body fragmentation channels contribute: $C+C_2$ for C_3^+, C_2+C_2 and $C+C_3$ for C_4^+. For C_5^+ and C_6^+ the final channels were also characterized by two-body fragmentation, but the specific channels were not identified because of limited mass resolution. It is being speculated whether cluster ions larger than C_6^+ may undergo recombination without dissociation. These clusters have a large heat capacity and a correspondingly lower temperature after electron capture. The decay of the intermediate neutral clusters may be influenced by infrared emission, which provides cooling and prevents dissociation.

DOI: 10.1103/PhysRevA.73.022712 PACS number(s): 34.80.Lx, 29.20.Dh, 52.20.Hv

I. INTRODUCTION

The dissociative recombination (DR) of small polyatomic ions is an important process in the chemistry of interstellar clouds, planetary atmospheres, and many laboratory plasmas. Experimental studies have been motivated by their practical importance and by a desire to understand the underlying dynamics of the process itself. A theoretical description of DR with diatomic ions is emerging, but DR of tri- and polyatomic ions remains a difficult theoretical problem. A well-known example is the dissociative recombination of the H_3^+ ion, which is viewed as a particularly important process for astrophysical reasons, and because H_3^+ is the simplest triatomic ion. Despite the fact that H_3^+ has received early attention both experimentally [1] and theoretically [2], it was only quite recently that Greene and collaborators found that the Jahn-Teller effect, which couples electronic and vibrational degrees of freedom, was essential to understanding the DR of H_3^+ [3]. The DR of many other and more complex polyatomic ions has been studied in recent times at heavy-ion storage rings, for example, H_2O^+ and H_3O^+ [4] and CO_2^+ [5]. Polyatomic hydrocarbons that contain several carbon atoms have also been studied in several experiments [6].

Small carbon clusters have received great attention after the discovery of the C_{60} fullerenes and the occurrence of small clusters in the interstellar medium and in carbon stars. C_3, for example, has appeared in the atmospheres of cool stars. C_3 may also be a critical link in the formation of soot in flames [7]. Pure carbon chains have been linked to the formation of circumstellar grains [8] and may be involved in the formation of diffuse interstellar bands [9]. A general review on small carbon clusters can be found in Ref. [10].

Here we report on the formation of carbon atoms and carbon molecules upon dissociative recombination of small carbon cluster cations. Dissociative recombination involves inverse ionization, and hence energy is released when an electron recombines with a C cluster cation. The energy is normally used to fragment the neutral intermediate into various channels like

$$C_n^+ + e^- \rightarrow C_i + C_j, \tag{1}$$

where i and j are integers ($i+j=n$).

It is generally found that while the cross sections do not vary much for the DR of such cations, the branching ratios between various dissociation patterns vary significantly. The outcome clearly depends on the potential-energy surfaces of the excited state which determine the dissociation dynamics. Unfortunately, it is a rather complex task to calculate all potential-energy surfaces and the relevant couplings, and a statistical approach may seem more feasible. Strasser *et al.* [11] have presented a semiclassical model where energy and momentum conservation define a phase-space region within which a uniform phase-space distribution applies. This approach seems best at high energy where specific molecular structure is of little importance.

We are dealing here with small C clusters with 3–6 atoms, and the number of degrees of freedom is between 4 and 12. The excess energy after electron capture (recombination) is of order 10 eV, and the excess energy per vibrational mode only about 1–3 eV. This is not a high energy compared to the dissociation energy (C-C bond), which is typically about 5 eV, and we expect that energy barriers along specific reaction coordinates will play a role. It may thus be more appropriate to calculate the probability for concentration of sufficient energy in a certain mode (reaction coordinate) to overcome a critical energy barrier [12]. We discuss this approach after having discussed the experimental technique and presented the results.

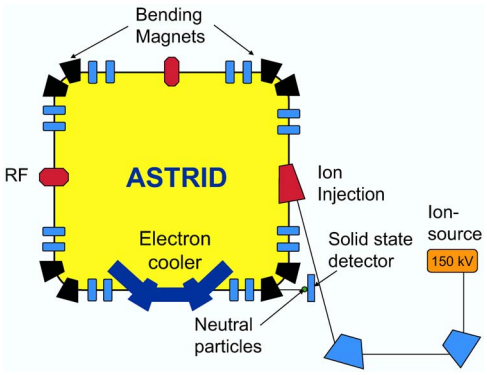

FIG. 1. (Color online) The ASTRID storage ring.

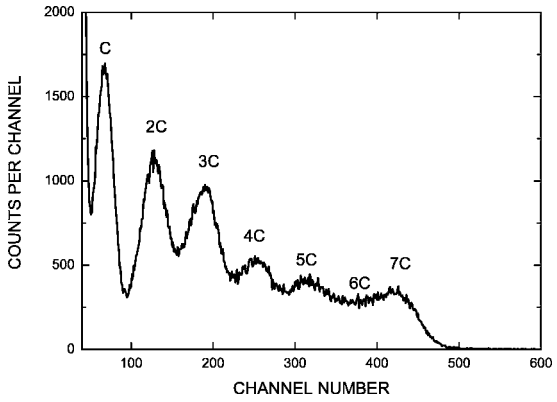

FIG. 2. Mass spectrum of collisionally induced fragments of C_7^+ stored in ASTRID. The data were recorded by the high-resolution detector SSD_2.

II. EXPERIMENTAL TECHNIQUE

Details of the experimental technique have been described previously [13] and only a brief description is given here with emphasis on the special circumstances that are encountered when rather heavy ions are considered. The experiment was conducted at ASTRID (Aarhus storage ring, Denmark) at the University of Aarhus. The carbon clusters were produced using two different ion sources located on a 150 kV preacceleration platform. For the smaller-size carbon cluster of C_3 and C_4, the Nielsen ion source was used with butane gas and Ne buffer gas. Larger clusters could not be produced by the Nielsen source. Many gas combinations from available chemical gases or liquids with long (5–6) carbon chains were tried as well as an oven with graphite powder. We detected ions with masses equivalent to those of C_5, C_6, and C_7; however a careful analysis with a high-resolution silicon detector showed that they were not carbon clusters.

We succeeded in generating the required larger carbon cluster with an electron cyclotron resonance (ECR) ion source from GANIL/CIRIL [14]. The source was available as part of the LEIF network [15]. This source has been modified and used for producing C_{60}^{n+} beams [16]. The C_{60} was introduced into the source through an oven heated to 400–500 °C. The clusters were produced due to the breakdowns of the C_{60}^{n+} within the plasma of the source.

A few nanoamperes of C_5, C_6, and C_7 were extracted from this source. The preaccelerated cluster cations were injected into the ASTRID storage ring. The C_3, C_4, C_5, and C_6 cluster ions were further accelerated in ASTRID to energies of 3.914, 2.939, 2.335, and 1.954 MeV, respectively. Due to the increasing mass of the larger clusters and the finite ring rigidity, the final energy was decreased as the cluster size was increased. A cooling time in the order of 2 s was applied after acceleration to stabilize the beam orbit. The time also enabled thermal relaxation of excited states in the clusters. In one of the straight sections of the ring (see Fig. 1), the ion beam was merged with the electron-beam of the electron-cooler device. The relative energy between the ion beam and the electron beam was tuned by changing the electron-beam energy. The electron-beam energy, angle, and overlap were optimized to give the strongest DR signal compared to the background from residual-gas collisions. This was achieved by chopping the electron beam to get the DR signal as well as the background signal. After recombination, neutral products continuing according to their straight trajectories reached a large (6×4 cm^2) solid-state detector (SSD_1) located just after the bending magnet at the corner of the ring (see Fig. 1). The deposited energy in the solid-state detector is proportional to the fragment mass since all fragments have about the same velocity, and hence mass spectra are equivalent to energy spectra. A small detector SSD_2 was located just inside the bending magnet. This second detector was inserted outside the main beam trajectory to detect the actual energy of the neutral fragments with better energy resolution than the large SSD, and hence verify the actual molecular identity of the stored beam. This procedure was crucial when the Nielsen ion source was used, since mass selection only gave the mass equivalent to C_5 and C_6, but not necessarily the right atomic composition. As a test of the small detector (SSD_2), a beam of C_7 from the ECR ion source was injected into the ring. The large detector could not resolve the fragments while the small one (SSD_2) was able to discern the fragments as shown in Fig. 2.

The signal from the large detector (SSD_1) was collected by two multichannel analyzers (MCAs), where one measured the fragments while the electron beam was on, and the other while the electron beam was off (background). In the case of C_3 and C_4 the peaks in the energy spectrum were also collected by fast counters through single-channel analyzers that were tuned to each peak detected on SSD_1. This was done to reduce the counting dead time for the stronger beams. For C_5 and C_6 this method could not be applied due to lack of energy resolution. The counting rate, however, was so low that no significant dead time was imposed on the two MCAs.

The energy spectra for two heavier clusters (C_5^+ and C_6^+) as measured in SSD_2 are presented in Fig. 3. As can clearly be seen, the energy resolution is becoming moderate. This has three reasons: (1) The storage energy of the cluster ions is decreasing as the cluster size increases, as explained above, (2) more atoms in a cluster impose less separation between neighboring peaks, and (3) energy loss in the detector front dead layer is more severe for slow and heavy particles. This is particularly significant in the larger detector SSD_1 as will be shown in the next section.

In order to determine the branching ratio of the DR process a special grid technique is used where a grid with trans-

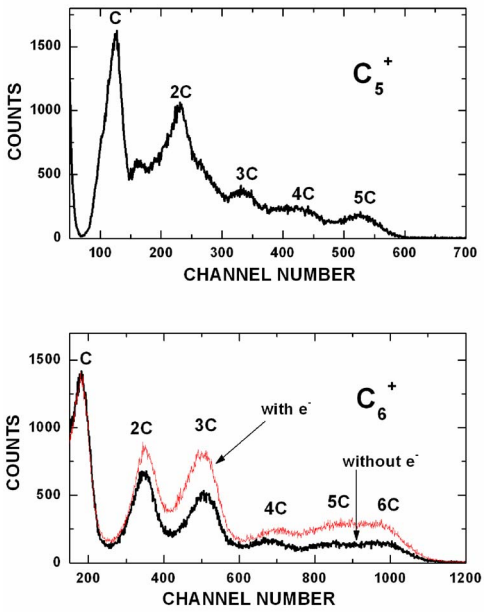

FIG. 3. (Color online) Mass spectrum of collisionally induced fragments of C_5^+ stored in ASTRID (upper spectrum) and of electron (signal) and collisionally (background) induced fragments of C_6^+ (lower spectra). The data were recorded by the high-resolution detector SSD_2.

mission probability T is inserted just in front of SSD_1. We use two grids with different transmissions (T=0.67 and 0.24). The full energy peak (containing the DR counts) in SSD_1 is then reduced in accordance with the DR branching ratio. If the DR process is purely a two-body dissociation process, the counts in the full energy peak are reduced by a factor T^2. If the DR process is a three-body dissociation process, the full energy peak is reduced by T^3. Any yield at the full energy peak between these two numbers shows that the DR process is a combination of two- and three-body dissociation. Such analysis will be used for the C_5 and C_6 data in the next section. A more complete analysis can be performed when the fragment energy spectrum from SSD_1 reveals peaks corresponding to fractional energies and masses as was the case for C_3 and C_4.

III. DATA ANALYSIS

A. C_3

Figure 4 illustrates the energy (equivalent to mass) distribution of fragments from dissociative recombination of C_3^+. Two energy spectra (from SSD_1) are shown, one with the electron beam on, and the other with the electron beam off. As can be seen, (1) mainly the full energy peak (C_3) results from the DR process, and (2) the low-energy peaks induced by the residual-gas collisions are slightly larger than the same peaks with the electron beam on. The reason for this is that the background MCA has fewer counts and therefore less dead time as explained above. Thus, for the detailed data analysis we only used the method based on the single-channel analyzers and not the MCA data.

The processes of concern are

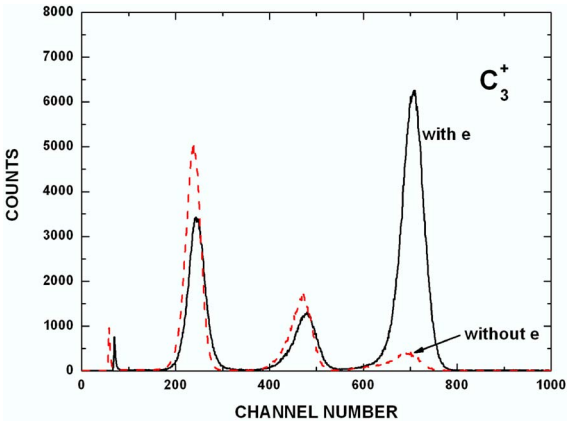

FIG. 4. (Color online) Mass spectrum of fragments of C_3^+ recorded by SSD_1.

$$C_3^+ + e^- \rightarrow \begin{cases} C_3 & (n_a), \\ C_2 + C & (n_b), \\ C + C + C & (n_c), \end{cases} \tag{2}$$

where n_i are the branching ratios. The branching ratios are computed by solving the following matrix equation:

$$N_E = (n_a T + n_b T^2 + n_c T^3) N_0,$$

$$N_{2E/3} = [n_b T(1-T) + n_c 3T^2(1-T)] N_0,$$

$$N_{E/3} = [n_b T(1-T) + n_c 3T(1-T)^2] N_0, \tag{3}$$

where N_E, $N_{2E/3}$, and $N_{1/3E}$ are the net counts (after background subtraction) in the counters that are set to the full energy peak and 2/3 and 1/3 of the full energy, respectively. N_0 is the total number of counts and the branching ratios are required to sum up to 1. When we solve the equations with data obtained with both grids we get

$$n_a = (0 \pm 0.1)\ \%\ ,$$

$$n_b = (100 \pm 0.2)\ \%\ ,$$

$$n_c = (0 \pm 0.1)\ \%\ . \tag{4}$$

Thus, only the two-body channel contributes to the DR of C_3^+ with zero energy electrons.

B. C_4

The results of the C_4^+ DR process are presented in Fig. 5. Two energy spectra (obtained on SSD_1) are shown, corresponding to electrons on and off. Again it can be seen that DR only contributes to the full energy peak (as expected since the process neutralizes the molecule). The fragment peaks as well as a small part of the full energy peak are due to residual-gas collisions. Here, similar to the C_3 analysis, only data from the counters were used, although the MCA dead time is much smaller due to the lower beam intensity. The DR processes that were considered are

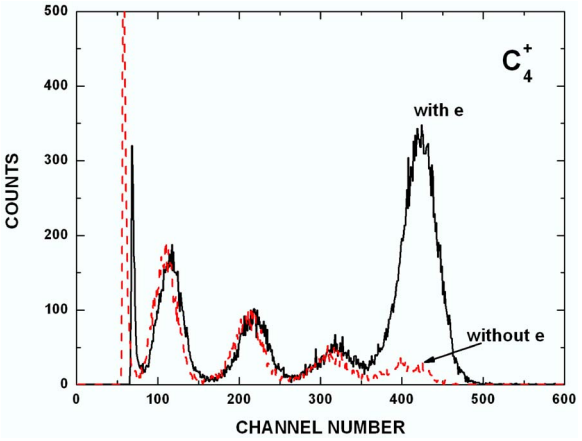

FIG. 5. (Color online) Mass spectrum of fragments of C_4^+ recorded by SSD_1.

$$C_4^+ + e^- \rightarrow \begin{cases} C_2 + C_2 & (n_a), \\ C_3 + C & (n_b), \\ C_4 & (n_c), \\ C_2 + C + C & (n_d). \end{cases} \tag{5}$$

The branching ratios are computed by solving the following matrix equation:

$$N_E = (n_a T^2 + n_b T^2 + n_c T + n_d T^3) N_0,$$

$$N_{3E/4} = [n_b T(1-T) + n_d 2T^2(1-T)] N_0,$$

$$N_{E/2} = [n_a 2T(1-T) + n_d T(1-T)] N_0,$$

$$N_{E/4} = [n_b T(1-T) + n_d 2T(1-T)^2] N_0, \tag{6}$$

where N_E, $N_{3E/4}$, $N_{E/2}$, and $N_{E/4}$ are the net counts (after background subtraction) in the counters that accumulate in the full energy peak and 3/4, 1/2, and 1/4 of the full energy peak, respectively (see Fig. 5). The results of solving the matrix equation with both grids are

$$n_a = (39 \pm 3)\ \%\ ,$$

$$n_b = (61 \pm 3)\ \%\ ,$$

$$n_c = (0 \pm 0.2)\ \%\ ,$$

$$n_d = (0 \pm 0.2)\ \%\ . \tag{7}$$

Only two-body dissociation is thus involved in the DR process of C_4^+. If we assume a linear chain structure of the C_4^+ ion, the result shows that the middle C-C bond breaks with a ~40% probability and each of the end C-C bonds breaks with a probability of ~30%. (The two end bonds result in a total branching ratio of ~60% for channel *b*.)

C. C_5 and C_6

The DR process of C_5^+ and C_6^+ was detected by SSD_1 with poor energy resolution due to the small energy per C atom of 467 and 326 keV, respectively. The resolution was not good enough to distinguish between the full energy peak and fragment peaks. In the data analysis one single peak (the full energy peak) was fitted to a single Gaussian in the case with no grid in front of the detector. Fits with three Gaussians were done to the SSD_1 spectra when grids were inserted. We then calculated the area of the fitted full energy peaks with background subtraction and the normalized ratio between the peak with grid and without grid. Since each spectrum was taken at different times, a special normalization procedure was applied to verify that the number of ions in the ring was correctly known. During each injection and storage period an additional measurement was undertaken with a pickup electrode and a spectrum analyzer. The beam intensity of each injection was measured using the electrode in a fixed time after the injection. The spectra with grids in front of the detector were measured with more injections in order to have better statistics. The actual damping due to insertion of a grid was calculated using the beam-normalization procedure described above. The damping owing to the finite transmission was for C_5, grid 1, 0.49±0.05 and grid 2, 0.08±0.02; for C_6, grid 1, 0.40±0.07 (for grid 2 satisfying fits were not possible). The normalized ratios (damping) between the full energy peak with a grid and without a grid are equal to T for no dissociation, T^2 for two-body fragmentation, and T^3 for three-body fragmentation. T, T^2, and T^3 are equal to 0.67, 0.45, and 0.3 for grid 1, and 0.24, 0.058, and 0.014 for grid 2, respectively. Therefore the results are consistent only with a two-body dissociation process. The actual fragmentation channels may be C_2+C_3 and C+C_4 for C_5^+ and C_3+C_3, C_2+C_4, and C+C_5 for C_6^+.

IV. DISCUSSION

In the following we will assume that mainly linear carbon cluster cations are present in the ion beam for the cluster sizes considered here. This assumption is justified by previous ion-reactivity studies [17]. All the branching ratios obtained in the present study show the same trend; only one C-C bond is broken in the DR process involving zero-energy electrons. The reason is that the neutral cluster after recombining with a zero-energy electron does not have enough energy to efficiently break more than a single C-C bond. This is different from many other large molecules especially those with many bonds involving hydrogen [4,6]. An upper limit of the available energy can be calculated using known data for neutral carbon cluster ionization potentials and their dissociation energies [18]. These energies are plotted in Fig. 6. The difference between the "ionization" curve and the "dissociation" curve indicates an upper limit of the molecular excitation energy after the DR process since some energy will go into kinetic energy of the fragments. The difference is plotted in Fig. 6 (triangular points). For C_3-C_6 this energy is about 5–6 eV, which is just barely enough to break another C-C bond. It is interesting to see that for C_7 the energy is less than 1 eV which is not enough to break another C-C bond. Actually, there is hardly enough energy for one dissociation, and one might speculate if DR of C_7^+ may produce a neutral C_7 molecule with no dissociation.

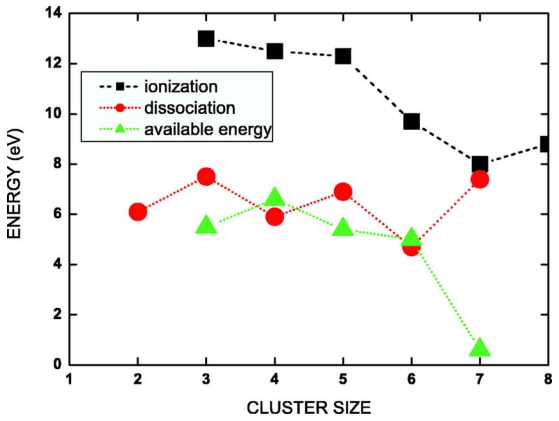

FIG. 6. (Color online) The ionization (squares) and dissociation (circles) energies of neutral carbon clusters as a function of cluster size. The available energy after dissociation is also shown (triangles).

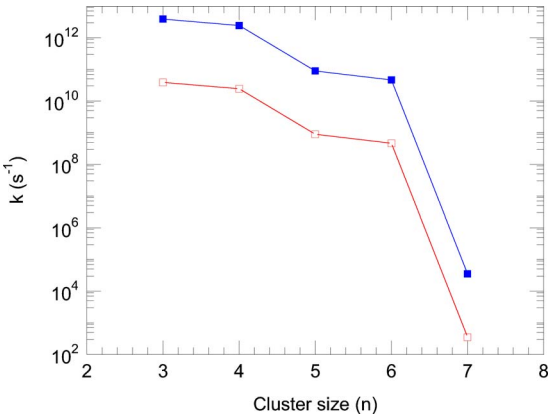

FIG. 7. (Color online) The calculated decay rate for dissociation of the C_n clusters as a function of n. $A=10^{14}$ (solid points) and 10^{12} s^{-1} (open points).

To estimate the stability after recombination we take a statistical approach. We assume full (i.e., fast) conversion of electronic energy into the nuclear vibrations, and calculate the decay time for spontaneous dissociation (unimolecular dissociation) after electron capture by applying the Arrhenius expression for the decay constant k [12]:

$$k(E) = A\exp[-E_a/k_B(T - E_a/2C)], \tag{8}$$

where A is the preexponential factor, E_a the activation energy for dissociation, and k_B Boltzmann's constant. The temperature T is related to the excitation energy E through the microcanonical caloric curve, and C is the derivative with respect to temperature of $E(T)$. We are here concerned with rather high temperatures, and C is approximated by the asymptotic value $(3N-6)k_B$, where N is the number of atoms in the molecule. The term $-E_a/2C$ is the finite-heat-bath correction which accounts for the fact that the effective decay temperature is the average of the microcanonical temperatures in the initial (undissociated) and final (dissociated) states [12]. The statistical approach outlined above has successfully been used to describe the delayed dissociation after photoabsorption for a number of organic chromophore molecules [19].

The calculated rates as a function of cluster size (n) are shown in Fig. 7. The effective temperatures become quite high after electron capture: ~4000 K for C_7 and ~27 000 K for C_3. Consequently, the decay is rather fast, in particular for the small clusters, despite the fact that the dissociation energy is high (5–6 eV). For C_7, however, the lifetime approaches the millisecond time scale and radiative cooling might start to compete with particle emission [20]. For even larger clusters it is possible that the clusters cool by infrared emission, which would eventually prevent dissociation; this remains to be established experimentally.

V. CONCLUSION

In conclusion we have determined branching ratios for the fragmentation of carbon clusters after electron capture. For all the studied systems (C_3–C_6) only two-body dissociation is observed. In the case of C_4^+, the final channels C_2+C_2 and C_3+C had branching ratios of about 40 and 60 %, respectively, corresponding to a 30% probability for C-C bond breakage at the ends and 40% probability for C-C bond breakage at the center bond of linear C_4. We applied a statistical approach and the Arrhenius expression for the decay constant, and we make the prediction that owing to the large heat capacity, the fragmentation may become very slow for large carbon clusters, provided that the internal conversion of electronic energy into the vibrations is fast.

ACKNOWLEDGMENTS

This work was supported by the Danish Natural Science Research Council (Grant No. 21-03-0330) and through the program "Transnational Access to Major Research Infrastructures," Contract No. HPRI-CT-2001-00122.

[1] For reviews and highlights, see M. Larsson *et al.*, Phys. Rev. Lett. **70**, 430 (1993); G. Sundstrøm *et al.*, Science **263**, 785 (1994); M. J. Jensen *et al.*, Phys. Rev. A **63**, 052701 (2001); B. J. McCall *et al.*, Nature (London) **422**, 500 (2003); L. Lammich *et al.*, Phys. Rev. Lett. **91**, 143201 (2003).

[2] See, for example, A. E. Orel and K. C. Kulander, Phys. Rev. Lett. **71**, 4315 (1993); I. F. Schneider, A. E. Orel, and A. Suzor-Weiner, *ibid.* **85**, 3785 (2000); A. E. Orel, I. F. Schneider, and A. Suzor-Weiner, Philos. Trans. R. Soc. London, Ser. A **358**, 2445 (2000).

[3] V. Kokoouline and C. H. Greene, Phys. Rev. Lett. **90**, 133201 (2003); V. Kokoouline and C. H. Greene, Phys. Rev. A **68**,

012703 (2003); V. Kokoouline, C. H. Greene, and B. D. Esry, Nature (London) **412**, 891 (2001).
[4] L. H. Andersen *et al.*, Phys. Rev. Lett. **77**, 4891 (1996); L. Vejby Christensen *et al.*, Astrophys. J. **483**, 531 (1997); M. J. Jensen *et al.*, *ibid.* **543**, 764 (2000); R. Thomas *et al.*, Phys. Rev. A **66**, 032715 (2002).
[5] K. Seiersen *et al.*, Phys. Rev. A **68**, 022708 (2003); A. A. Viggiano *et al.*, J. Chem. Phys. **122**, 226101 (2005).
[6] W. D. Geppert *et al.*, Astrophys. J. **613**, 1302 (2004); W. D. Geppert *et al.*, Int. J. Mass. Spectrom. **237**, 25 (2004); A. Ehlerding *et al.*, Phys. Chem. Chem. Phys. **6**, 949 (2004); A. Ehlerding *et al.*, J. Phys. Chem. A **107**, 2179 (2003); S. Kalhori *et al.*, Astron. Astrophys. **391**, 1159 (2002); G. Angelova *et al.*, Int. J. Mass. Spectrom. **235**, 7 (2004); G. Angelova *et al.*, *ibid.* **232**, 195 (2004); J. B. A. Mitchell *et al.*, *ibid.* **227**, 273 (2003).
[7] A. G. Gaydon and H. G. Wolfhard, *Flames* (Chapman and Hall, London, 1978).
[8] H. W. Kroto, J. R. Heath, S. C. O'Brian, R. F. Curl, and E. E. Smalley, Astrophys. J. **314**, 352 (1987).
[9] A. E. Douglas, Nature (London) **269**, 130 (1977).
[10] A. V. Orden and R. J. Saykally, Chem. Rev. (Washington, D.C.) **98**, 2313 (1998).
[11] D. Strasser, J. Levin, H. B. Pedersen, O. Heber, A. Wolf, D. Schwalm, and D. Zajfman, Phys. Rev. A **65**, 010702(R) (2001).
[12] J. U. Andersen, E. Bonderup, and K. Hansen, J. Chem. Phys. **114**, 6518 (2001).
[13] M. J. Jensen *et al.*, Phys. Rev. A **60**, 2970 (1999).
[14] P. Jardin *et al.*, Rev. Sci. Instrum. **73**, 789 (2002).
[15] Project reference HPRI-CT-1999-40012.
[16] L. Maunoury *et al.*, Rev. Sci. Instrum. **75**, 1884 (2004).
[17] S. W. McElvany, B. I. Dunlap, and A. O'Keefe, J. Chem. Phys. **86**, 715 (1987).
[18] M. B. Sowa-Resat, P. A. Hintz, and S. L. Anderson, J. Phys. Chem. **99**, 10736 (1995).
[19] See, for example, S. B. Nielsen *et al.*, Phys. Rev. Lett. **87**, 228102 (2001); S. B. Nielsen *et al.*, *ibid.* **91**, 048302 (2003); L. H. Andersen *et al.*, Phys. Chem. Chem. Phys. **6**, 2617 (2004).
[20] K. F. Freed, T. Oka, and H. Suzuki, Astrophys. J. **263**, 718 (1982).